THE JOURNAL OF PHYSICAL CHEMISTRY C

pubs.acs.org/JPCC Article

Ultrafast Dynamics of Long-Lived Bound Triplet Pair Generated by Singlet Fission in 6,13-Bis(triisopropylsilylethynyl) Pentacene

Zilin Zhou, Lin Ma,* Deqiang Guo, Xin Zhao, Cheng Wang, Dabin Lin, Fangteng Zhang, Jiahua Zhang, and Zhaogang Nie*

Cite This: J. Phys. Chem. C 2020, 124, 14503−14509 Read Online

ACCESS | Metrics & More | Article Recommendations | Supporting Information

ABSTRACT: Singlet fission (SF) converts a singlet exciton into two triplet excitons and holds great potential in the photovoltaic field. The triplet pair state is proposed to play an important role in SF. However, the existence and character of the triplet pair state are still ambiguous to date. In this study, we directly observed the ultrafast formation of the long-lived bound triplet pair state in 6,13-bis-(triisopropylsilylethynyl) pentacene polycrystalline film using sub-10-fs broadband transient absorption spectroscopy. The triplet pair state has strong absorption in the near-infrared region and shows distinct dynamic characteristics. It shows faster formation and relaxation compared to free triplet states. Diffusion-limited triplet−triplet annihilation was proved to be the major relaxation channel for both free triplets and bound triplet pairs. Moreover, the larger constraint coefficient obtained from triplet−triplet annihilation of the bound triplet pair state reveals the inherent coupling nature between its two constituent triplets.

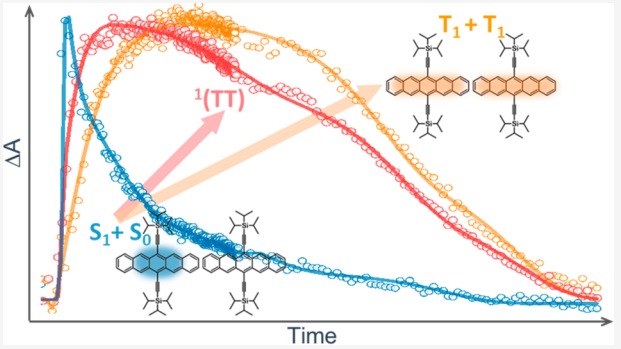

INTRODUCTION

Singlet fission (SF) is a spin-conserving process in which a high-energy singlet exciton splits into two low-energy triplet excitons in organic multichromophoric systems.[1,2] In recent years, it has attracted increasing attention in the field of photovoltaics, owing to its potential to circumvent the Shockley−Queisser limit for single-junction solar cells.[2−4] The singlet fission mechanism can be briefly described as follows:[3,4]

$$S_1 + S_0 \rightleftharpoons {}^1(TT) \rightleftharpoons {}^1(T\cdots T) \rightleftharpoons T_1 + T_1$$

In this process, a chromophore in the ground state (S_0) is excited to the first excited singlet state (S_1) and interacts with an adjacent chromophore in the ground state (S_0) to produce a triplet pair state $^1(TT)$. The triplet pair state is initially tightly coupled with an overall singlet spin multiplicity.[1] The coupling weakens with separation of the two triplets $^1(T\cdots T)$ until dissociation into two free triplet excitons (T_1).[5] Previous experimental studies mainly focus on the ultrafast singlet decay and triplet generation, thus confirming SF is the underlying mechanism. For the triplet pair state, direct experimental characterizations on its formation and dissociation processes are challenging because of its ultrashort lifetime and strong spectral overlap with singlet or triplet states.[6,7] Therefore, the role of the triplet pair state in SF remains ambiguous.[3,8] On one hand, it is considered an intermediate between singlet decay and triplet formation.[9,10] On the other hand, recent reports suggest that there are also bound triplet pair states that decay nonradiatively to ground states instead of dissociating into free triplets.[11,12] Revealing the formation and relaxation processes of the triplet pair state is critical to understanding the SF mechanism and fully utilizing the exciton multiplication merit of SF in optoelectronic devices.

TIPS-pentacene (6,13-bis(triisopropylsilylethynyl) pentacene), a soluble derivative of pentacene, is a famous SF prototype material, with SF proceeding on the sub-100-fs time scale.[13−15] However, the existence and role of the triplet pair state in SF of TIPS-pentacene have been controversial, until now. SF processes in TIPS-pentacene film or crystal were widely studied by femtosecond transient absorption (TA) spectroscopy with visible spectral detection range. The obtained TA spectral features contain a positive photoinduced absorption (PIA) TA signature at a shorter wavelength range (<500 nm), which is assigned to the excited singlet-state transition ($S_1 \rightarrow S_n$), and a PIA band around 530 nm, which is attributed to the triplet-state absorption ($T_1 \rightarrow T_n$).[13,14,16] Excited-state dynamics of TIPS-pentacene film is mainly

Received: April 22, 2020
Revised: June 9, 2020
Published: June 9, 2020

https://dx.doi.org/10.1021/acs.jpcc.0c03566
J. Phys. Chem. C 2020, 124, 14503−14509

described by an ultrafast decay of excited singlet states accompanied by a rise of triplet states, confirming the occurrence of SF. There are also a few TA studies carried out in the near-infrared (NIR) region, where a broad TA band in the range of 780−1000 nm was observed. However, the origin of this NIR band is still disputable: Yost et al.[17] and Musser et al.[14] assigned this TA band to the absorption of triplet states ($T_1 \rightarrow T_2$). Herz et al.[13] attributed this band to a higher vibrational level triplet state since its rise time is slightly shorter than that of the visible band (530 nm). However, Yong et al.[18] and Stuart et al.[11] attributed this TA band to the absorption of triplet pair states, which decay nonradiatively back to ground states instead of dissociating into free triplets.

In this work, we systematically studied the spectral and dynamic characteristics of the long-lived triplet pair state in TIPS-pentacene film by using sub-10-fs broadband transient absorption spectroscopy. Apart from the known free triplet states inducing a visible TA band around 530 nm, a broad NIR PIA band at around 860 nm was observed with distinct dynamics. It shows faster formation and relaxation compared to free triplets. Excitation-intensity-dependent TA dynamics, global analysis, and theoretical calculation suggested this broad NIR TA band mainly originates from the bound triplet pair state, which does not dissociate into free triplets.

EXPERIMENTAL SECTION

Sample Preparation. TIPS-pentacene powder was purchased from Ossila Ltd. (purity >99%). The chlorobenzene solution was purchased from Sigma-Aldrich (purity >99.5%). All chemicals were used as received without further purification unless otherwise stated. The glass substrate was cleaned in 1% Hellmanex III solution for 10 min and in IPA solution for 10 min, followed by a 30 min treatment in a UV-ozone cleaner. TIPS-pentacene in chlorobenzene solution (concentration of 50 mg/mL) was stirred for 8 h and spin-coated on the precleaned glass substrate at a rate of 3000 rpm for 30 s. The obtained film was then annealed on a hot plate at 80 °C for 20 min.

Steady-State Characterization. The steady-state absorption spectra of TIPS-pentacene film and diluted solution in chlorobenzene (1 mg/mL) were measured with a Shimadzu UV 3600 Plus spectrometer. The X-ray diffraction pattern of the TIPS-pentacene film was collected using a Bruker D8 Advance X-ray diffractometer (Bruker AXS, Germany), with Cu Kα irradiation at 40 kV and 40 mA, and the diffraction angle scan range was 3°−70°. Step scan mode was used during the XRD analysis with a step size of 0.02 and a dwell time of 0.8 s for each step.

Sub-10-fs Broad Band Transient Absorption Spectroscopy. The broadband sub-10-fs TA spectra were collected using an amplified Ti:sapphire laser system (Solstice Ace35F1K HP, Spectra Physics), with an output of 800 nm at 1 kHz repetition rate, 35 fs pulse width, and output power of 6 W. Broadband pulses (480−970 nm) are produced by spectrally broadening the output 800 nm pulse in a helium-filled hollow-core fiber. More details were reported previously.[19] Pulse compression by the chirped mirrors (UltraFast Innovations, Design PC1332) yields transform-limited pulses of 6 fs duration. The autocorrelation trace of pump and probe pulses was performed using a 10 μm BBO crystal (Caston Inc.), as shown in Figure S1 (Supporting Information). The broadband pulses were split into two beams by a beam splitter. The stronger beam was used as the broadband excitation pump pulse, and the weaker one was used as a probe beam. A combination of the half wave plate and a broadband polarizer controls the power and polarization of both beams. The polarization of the pump (vertical) and probe (horizontal) beams are set orthogonally to minimize the coherent artifacts. A computer-controlled, piezo-driven translation stage (Physik Instrumente, N-565.360) incorporated with a long traveling path translation stage (Newport, M-IMS1200LM) were placed in the pump beam arm to generate a time delay between the pump and probe pulses with a 1 fs time delay precision and an 8 ns time window.

RESULTS AND DISCUSSION

TIPS-pentacene film with a thickness around 180 nm was spin-coated on a glass substrate followed by thermal annealing. Steady-state absorption spectra of a TIPS-pentacene film and a diluted solution in chlorobenzene are shown in Figure 1a.

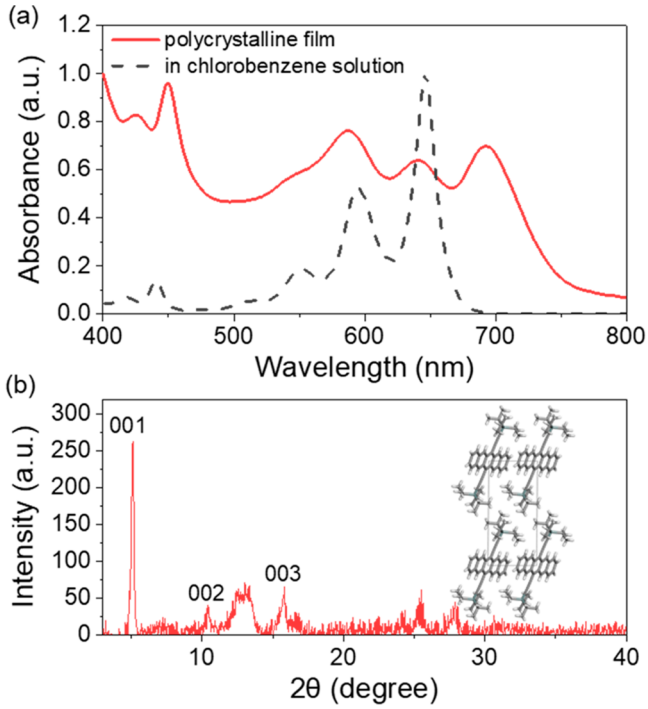

Figure 1. (a) Steady-state absorption spectra of TIPS-pentacene film (red solid line) and dilute solution in chlorobenzene (black dash line). (b) X-ray diffraction pattern of TIPS-pentacene film.

Compared to the solution, there is an additional absorption peak around 700 nm, indicating good crystallinity in the TIPS-pentacene film.[16,20,21] XRD pattern (Figure 1b) shows sharp diffraction angles at 5.07°, 10.5°, and 15.9°, corresponding to (001), (002), and (003) planes in the crystallographic *c*-direction, respectively.[16,22] The relatively broader diffraction peak around 13.5° is related to molecular packing along other crystallographic directions induced by thermal annealing.[16]

Transient absorption spectra of TIPS-pentacene film (Figure 2a) were measured by a hollow-core fiber compressor system described in the Experimental Section. Both pump and probe beams span the wavelength range from 480 to 970 nm, with a temporal bandwidth of 6 fs (Figure S1). The main features in the TA spectra are as follows: (i) three weak negative ground-state bleaching (GSB) bands with peak positions at around 587, 645, and 695 nm, which correspond well with the steady-

https://dx.doi.org/10.1021/acs.jpcc.0c03566
J. Phys. Chem. C 2020, 124, 14503−14509

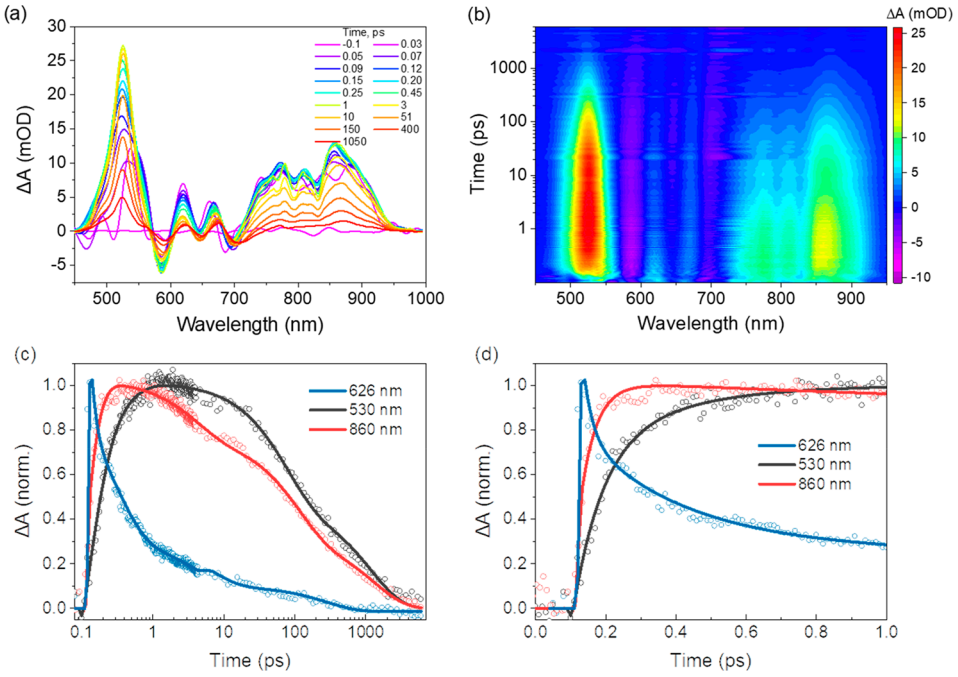

Figure 2. (a) Broadband TA spectra of TIPS-pentacene film. (b) 2D pseudocolor map of TA spectra as a function of probe wavelength and delay time between the pump and probe. TA kinetic traces at various probe wavelengths within time windows of (c) 6 ns and (d) the first 1 ps. (The time 0 is shifted to 0.1 ps in (b) and (c) to plot the time in log scale).

state absorption spectrum (Figure 1a, red curve); (ii) a positive photoinduced absorption (PIA) band at around 530 nm, which was concordantly attributed to the absorption from triplet states generated via the singlet fission process ($T_1 \rightarrow T_n$);[14,16,23] (iii) two small positive PIA bands with peaks located at around 620 and 670 nm undergo ultrafast decay, which are assigned to the excited singlet-state absorption ($S_1 \rightarrow S_n$);[6,12] (iv) a broad NIR PIA band with a maximum at around 860 nm spans the spectral region from 735 to 1000 nm. It is worthy to note that the negative GSB are highly overlapped with the positive PIA signal in the TA spectra shown in Figure 2a. Therefore, the real bandwidths and peak positions of the corresponding GSB or PIA bands could be much broader and slightly shift from the above suggested values. In contrast to the well-known visible PIA band, the origin of the NIR PIA band remains elusive. First of all, the NIR PIA band is often neglected because of the visible spectral bandwidth limitation in conventional TA setups.[14,20] As mentioned previously, only a few studies have reported on this TA band. Yost et al.[17] and Herz et al.[23] assigned it to triplet-state absorption, more specifically, the $T_1 \rightarrow T_2$ transition. However, Yong et al.[18] and Stuart et al.[11] attributed this TA band to the absorption of triplet pair states. Figure 2b shows a pseudocolor (ΔA) representation of the TA spectra in the TIPS-pentacene film. It can be seen that the broad NIR PIA band shows different dynamics compared to the visible PIA band: the overall rise and decay times of the NIR PIA band are shorter than those of the visible PIA band. A preliminary analysis is performed by comparing the TA kinetics at three feature probe wavelengths (λ_{probe}) of 530, 626, and 860 nm (Figure 2c). A global analysis on the whole TA spectra is performed later on. As an initial evaluation, an exponential kinetics model was used to obtain the ultrafast rise and decay times at various probe wavelengths. However, it is noteworthy that a diffusion-limited triplet−triplet annihilation model is proved to be the more suitable fitting model based on the intensity-dependent kinetics discussed later. Therefore, here, we focus only on the sub-100-fs time components shown in Table S1. The TA kinetics at λ_{probe} = 626 nm shows an ultrafast decay component of τ_1 = 30 ± 10 fs, which is due to the ultrafast decay of the singlet excited-state S_1 via singlet fission. The formation time τ_{rise} = 45 ± 2 fs at λ_{probe} = 860 nm is about 2 times faster than that of λ_{probe} = 530 nm (τ_{rise} = 80 ± 10 fs). The 80 fs rise time at 530 nm is in good agreement with the previously reported triplet formation time.[14,18,23] Little attention was paid to the 860 nm TA band, which was either assigned to the lower triplet transition or the equilibrium between triplet and triplet pairs.[24] Here, ultrafast formation times are clearly resolved with sub-10-fs time resolution, as shown in Figure 2d. Therefore, we can conclude that, beside the free triplet state, there is an additional transient state formed from the excited singlet-state S_1. Time-dependent density functional theory (TDDFT) calculations were also performed to study the triplet-state absorption. Vertical excitation energies with respect to the T_1 state and corresponding oscillator strengths for the TIPS-pentacene molecule were calculated as described in the Supporting Information. The obtained T_1 absorption spectrum and detailed calculation results are shown in Figure S3 and Table S2 (Supporting Information). The major triplet excited-state transition locates at 526.3 nm with an oscillator strength of 0.55. It is in excellent agreement with the visible TA band location from the TA experiment. In the NIR region, there is a very weak transition of $T_1 \rightarrow T_2$ at 945.7 nm with an oscillator strength of only 0.01, which is 50 times weaker than the visible-range transition at 526.3 nm. The triplet transition dipole moments are along the long axis of the pentacene backbone. These calculation results are consistent with previous theoretical calculations[25] and experimental results[26] for a pentacene molecule or solution. Khan et al. also reported

https://dx.doi.org/10.1021/acs.jpcc.0c03566
J. Phys. Chem. C 2020, 124, 14503−14509

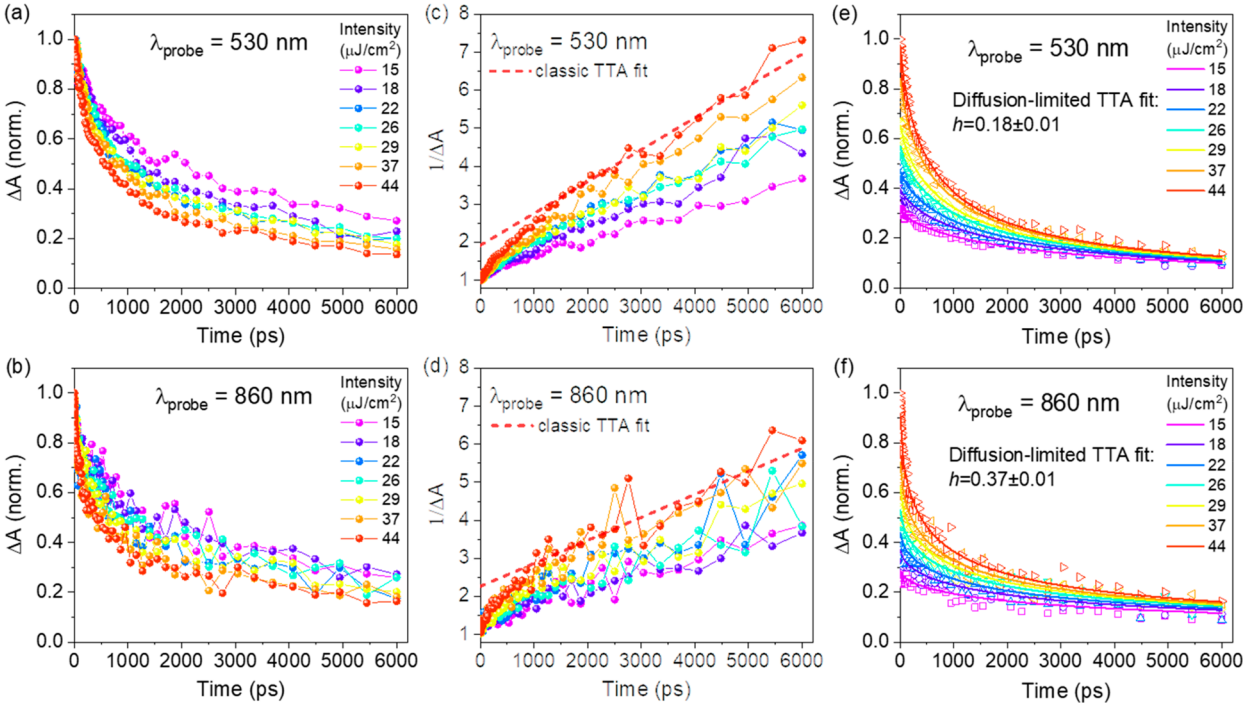

Figure 3. Excitation-intensity-dependent ΔA decay traces of (a) 530 nm and (b) 860 nm. ΔA^{-1} decay traces of (c) 530 nm and (d) 860 nm (The red dash lines are classic TTA fitting results). Global fitting results based on diffusion-limited TTA model for TA kinetics of (e) 530 nm and (f) 860 nm under various excitation intensities. (All decay curves were divided by the maximum TA magnitude at an excitation intensity of 44 μJ/cm^2.)

that a free triplet absorbs mainly in the visible range, while the triplet pair absorbs in both the visible and the NIR range via theoretical calculations for the pentacene crystal.[27] In our recent work, in a TIPS-pentacene/perovskite ($CH_3NH_3PbI_3$) bilayer structure, we demonstrated the presence of ultrafast electron transfer from the NIR TA band of TIPS-pentacene to the conduction band of perovskite, whereas the electron transfer from the visible TA band is on a much slower time scale.[28] It indicates that the final-state energy of the NIR TA band is higher than that of the visible TA band. Therefore, on the basis of the above experimental and theoretical results, we attribute the main origin of the NIR PIA band to the bound triplet pair states (denoted as ^{1}(TT) hereafter) rather than free triplet states. It is worth mentioning that according to the later global analysis on all the TA spectra, there is indeed broad spectral overlap for T_1, ^{1}(TT), and S_1. However, for the sake of simplicity, we focus only on the dynamics at a single wavelength for the moment. The global analysis is discussed later after we obtain the kinetic model for different TA bands.

The TA dynamics were further investigated via excitation-intensity-dependent TA measurements (Figure 3). The excitation intensities applied were in the linear-dependent range to avoid higher order nonlinear effect (Figure S4). In general, the relaxation kinetics of both free triplets (530 nm) and the bond triplet pair (860 nm) become faster with increasing excitation intensity (Figure 3a,b). In singlet fission, triplet generation is often followed by recombination assisted by triplet−triplet annihilation (TTA), which shortens the lifetime of the triplet states and should be suppressed to achieve high photoconversion efficiency. TTA is a bimolecular recombination process that follows the second-order recombination as shown in eq 1:

$$\frac{dn(t)}{dt} = -kn(t)^2 \tag{1}$$

$$n(t) = \frac{n(0)}{1 + kn(0)t} \tag{2}$$

$$\frac{1}{n(t)} = \frac{1}{n(0)} + kt \tag{3}$$

where $n(t)$ is the triplet concentration at time t and k is the TTA rate constant. Equation 2 is the analytical solution of eq 1, where $n(0)$ is the triplet concentration at $t = 0$. Furthermore, $n(t)^{-1}$ will linearly depend on time t, described by eq 3. Therefore, we plotted the reciprocal TA magnitude (ΔA^{-1}) versus time as shown in Figure 3c,d. It is clearly seen that ΔA^{-1} shows a linear dependence at a longer time ($t \geq 1500$ ps), indicating that the predominant recombination channels for both T_1 and ^{1}(TT) are via bimolecular TTA instead of unimolecular triplet relaxation to the ground state. It is in agreement with previously reported TTA behavior on a nanosecond time scale in TIPS-pentacene film.[16] However, the classic TTA fitting (eq 1) is unsatisfactory in the shorter time range ($t < 1500$ ps), as indicated by the red dash lines in Figure 3c,d. One rate-determining process for TTA is the migration of two triplet excitons toward one another; that is, the exciton diffusion constant governs the magnitude of the TTA rate for triplet states.[29] Considering the polycrystalline nature of the TIPS-pentacene film, the triplets in the form of either free triplet T_1 or bound triplet pair ^{1}(TT) are spatially constrained on the microscopic level by phase or grain boundaries. Therefore, TTA in TIPS-pentacene film is expected to follow the fractal kinetics where the TTA rate k depends on time.[30] Thus, we introduce the time-dependent TTA rate coefficient $k(t)$ as described by eq 4:

https://dx.doi.org/10.1021/acs.jpcc.0c03566
J. Phys. Chem. C 2020, 124, 14503−14509

$$k(t) = k_0 t^{-h}, \quad 0 \le h \le 1 \tag{4}$$

$$\frac{dn(t)}{dt} = -k_0 t^{-h} n(t)^2, \quad 0 \le h \le 1 \tag{5}$$

where $k(t)$ is the instantaneous TTA rate coefficient. In a three-dimensional homogeneous free space, $h = 0$, resulting in a constant k_0, in agreement with the classic TTA model (eq 1). However, for diffusion-limited TTA reactions that occur in constrained fractal spaces, $h > 0$, resulting in a time-dependent $k(t)$.[30] Therefore, h is a factor correlated with the constraint level of triplet states. The diffusion-limited TTA model (eq 5) is obtained by replacing k with $k(t)$ and applied to fit the intensity-dependent TA decay traces at 530 and 860 nm. Compared to classic TTA, the diffusion-limited TTA model achieved a much better fitting (Figure S5). In addition, we normalized the TA decay curves under an excitation intensity of 44 μJ/cm^2 and rescaled all other TA decay curves with their intensity ratios to 44 μJ/cm^2. As shown in Figure 3e,f, satisfactory fitting was obtained by global fitting all TA decay curves under various excitation intensities using the diffusion-limited TTA model with shared k_0 and h. The obtained h factors are 0.18 and 0.37 for 530 and 860 nm, respectively. It indicates that, apart from geometrical constraints induced by grain or phase boundaries in the polycrystalline TIPS-pentacene film, triplet states in the form of a bound triplet pair have additional constraints compared to free T_1, which can be assigned to the coupling interaction between the two constituent triplet states in a bound triplet pair. The TTA for the bound triplet pair could take place between the constituent triplets within the triplet pairs, as well as between the triplet pair and free triplet.

On the basis of the above information, global fitting analyses of the TA data set in Figure 2 were performed according to the following model (eqs 6–9):

$$\frac{dn_1(t)}{dt} = -k_1 n_1(t) \tag{6}$$

$$\frac{dn_2(t)}{dt} = -k_2 n_2(t) \tag{7}$$

$$\frac{dn_{TT}(t)}{dt} = k_1 n_1(t) - k_3 t^{-h_1} n_{TT}(t)^2 \tag{8}$$

$$\frac{dn_T(t)}{dt} = k_2 n_2(t) - k_4 t^{-h_2} n_T(t)^2 \tag{9}$$

where $n_1(t)$ is the population of S_1, which converted to triplet pair ^{1}(TT), $n_2(t)$ is the population of the precursor state, which converted to free triplets T_1, $n_{TT}(t)$ is the population of ^{1}(TT), $n_T(t)$ is the population of T_1, k_1 is the formation rate constant of ^{1}(TT), k_2 is the formation rate constant of T_1, and k_3 and k_4 are the diffusion-limited TTA rates of ^{1}(TT) and T_1, respectively. h_1 and h_2 are the constraint factors, which are fixed at 0.37 and 0.18 for ^{1}(TT) and T_1, according to the intensity-dependent fitting results (Figure 3). The species-associated spectra and kinetics obtained from the global fits are presented in Figure 4. The global fit yields $k_1 = 33$ ps^{-1}, $k_2 = 12$ ps^{-1}, $k_3 * n_{TT}(0) = 0.61$ ps^{-1}, and $k_4 * n_T(0) = 0.014$ ps^{-1}. We are not able to obtain the absolute value of k_3 and k_4 here since the extinction coefficients for T_1 and ^{1}(TT) are unknown. It is highly possible that the precursor of the free triplet (n_2) is actually another triplet pair intermediate, which dissociates quickly into free triplets. However, the obtained spectra of n_1 and n_2 are highly structured because of the influence from a coherent artifact at an early time as shown in Figure S2 (Supporting Information), making it difficult to distinguish the actual spectral difference between n_1 and n_2. Nonetheless, this does not detract from comparisons between the free triplets and bound triplet pairs. The extracted spectra of T_1 and ^{1}(TT) show spectral overlap in both the visible and NIR range. Moreover, the spectrum of T_1 focuses more in the visible region and the spectrum of ^{1}(TT) has larger contribution and covers a broader range in the NIR region. It agrees with the theoretical calculations study in pentacene crystal, which reports that the free triplet absorbs mainly in the visible range, whereas the triplet pair absorbs in both the visible and NIR range.[27] However, it is noteworthy to mention that the contribution in the NIR region from the triplet pair state observed in our experiments is much larger than the theoretical prediction. Because of the spectral overlap in the NIR region from T_1 and ^{1}(TT), the TA kinetics at 860 nm presented in Figure 2c actually contains contributions from the slow T_1 and fast ^{1}(TT), which makes it exhibit a slower decay than the extracted kinetics of the ^{1}(TT) state (Figure 4b). Similarly, the TA kinetics at 626 nm (Figure 2c) decays more slowly compared to the extracted kinetics of S_1 because of the small overlap from the much slower T_1 and ^{1}(TT) in the visible range. We assign the different dynamics for the free triplet and the bound triplet pair to the different local packing structures presented in the TIPS-pentacene film.[16,21] Triplets are preferred to form at a local spot with a lower crystalline degree, whereas the bound triplet pairs are preferred to form at a local spot with better crystalline degree where triplets are not easy to diffuse apart because of the large intermolecular interaction. Similar observations were reported in the amorphous TIPS-pentacene/polymer nanoparticles, where half of the triplet pair states decayed to the ground state rather than dissociating into free triplets.[11] The formation rates

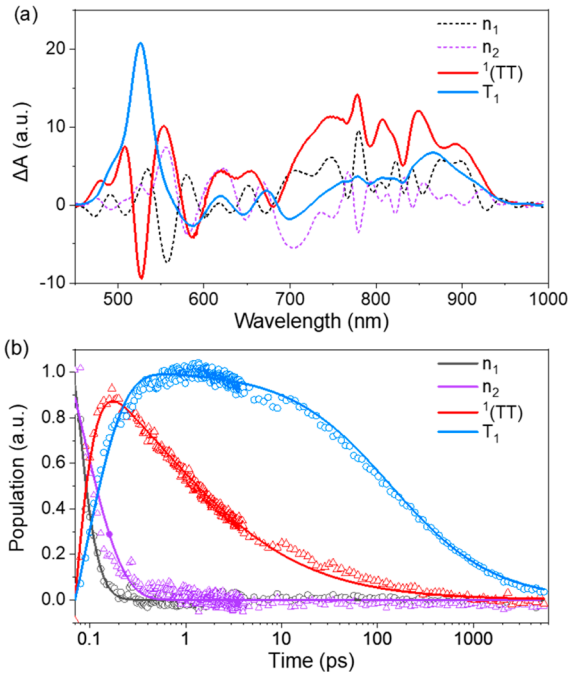

Figure 4. (a) Species-associated spectra and (b) kinetics obtained from global fitting of the TA data.

https://dx.doi.org/10.1021/acs.jpcc.0c03566
J. Phys. Chem. C 2020, 124, 14503−14509

of both triplet pairs are much slower than our results, which could be attributed to the closer molecular packing in the TIPS-pentacene polycrystalline film in our experiments compared to that in the amorphous nanoparticles.[11] The long-lived triplet pair observed in our experiments is not the precursor of free triplets; otherwise, it will show an ultrafast lifetime corresponding to the rise time of T_1. Instead, it survives much longer and competes with the free triplet formation. We could not distinguish the precursor triplet pair for free triplets because of the interference from the coherent artifact at an early time as shown in Figure S2 (Supporting Information). It has been reported that multielectron transfer (MET) from ^{1}(TT) via either sequential 1ET or concerted 2ET could be utilized to improve solar cell efficiency.[31,32] Therefore, utilization of the long-lived bound triplet pairs should be taken into consideration in future works to fully exploit the potential of singlet fission in boosting solar cell efficiency. Moreover, the long-lived bound triplet pair could also be applied in new areas such as quantum computing and quantum cryptography.[31,33]

CONCLUSIONS

In summary, the long-lived bound triplet pair state ^{1}(TT) generated via singlet fission in TIPS-pentacene film was verified via sub-10-fs broadband transient absorption spectroscopy. It has higher transition strength in the NIR range with distinct dynamic characteristics compared to that of the free triplet-state T_1. Its ultrafast formation time (45 fs) is about 2 times faster and the overall lifetime is slightly shorter than that of the free triplet state. Moreover, diffusion-limited triplet−triplet annihilation was demonstrated as the major relaxation channel for both T_1 and ^{1}(TT) via an excitation-intensity-dependent TA study. ^{1}(TT) undergoes faster TTA because of the inherent bound constraint between its two constituent triplets. Our results shed more light on the mechanism of singlet fission and suggest that it is necessary to differentiate SF efficiency from the triplet quantum yield in future studies. Moreover, inhibition of TTA and utilization of bound triplet pairs should be taken into consideration in future works to fully exploit the potential of singlet fission sensitizers in optoelectronic devices.

ASSOCIATED CONTENT

Supporting Information

The Supporting Information is available free of charge at https://pubs.acs.org/doi/10.1021/acs.jpcc.0c03566.

TA fitting parameters; theoretical calculation method; supporting Figures S1−S5 (PDF)

AUTHOR INFORMATION

Corresponding Authors

Lin Ma − *School of Physics and Optoelectronic Engineering, Guangdong University of Technology, Guangzhou 510006, China*; orcid.org/0000-0002-1815-6201; Email: malin@gdut.edu.cn

Zhaogang Nie − *School of Physics and Optoelectronic Engineering, Guangdong University of Technology, Guangzhou 510006, China*; Email: zgnie@gdut.edu.cn

Authors

Zilin Zhou − *School of Physics and Optoelectronic Engineering, Guangdong University of Technology, Guangzhou 510006, China*

Deqiang Guo − *School of Physics and Optoelectronic Engineering, Guangdong University of Technology, Guangzhou 510006, China*

Xin Zhao − *School of Physics and Optoelectronic Engineering, Guangdong University of Technology, Guangzhou 510006, China*

Cheng Wang − *School of Physics and Optoelectronic Engineering, Guangdong University of Technology, Guangzhou 510006, China*

Dabin Lin − *School of Physics and Optoelectronic Engineering, Guangdong University of Technology, Guangzhou 510006, China*

Fangteng Zhang − *School of Physics and Optoelectronic Engineering, Guangdong University of Technology, Guangzhou 510006, China*

Jiahua Zhang − *State Key Laboratory of Luminescence and Applications, CIOMP, Chinese Academy of Sciences, Changchun 130033, China*

Complete contact information is available at: https://pubs.acs.org/10.1021/acs.jpcc.0c03566

Notes

The authors declare no competing financial interest.

ACKNOWLEDGMENTS

We thank Prof. Zhimin Ao for his help with quantum chemistry calculations. This work was supported by the National Natural Science Foundation of China (Grant Nos. 11874125, 11704079, and 11774071), the Science and Technology Program of Guangzhou (Grant Nos. 201804010451 and 201904010104), the State Key Laboratory of Luminescence and Applications (Grant No. SKLA-2019-09), the Guangdong University Students Science and Technology Innovation Training Special Fund (Grant No. pdjh2019b0155), and the Guangdong Pearl River Talents Plan (Grant No. 2017GC010058).

REFERENCES

(1) Smith, M. B.; Michl, J. Singlet Fission. *Chem. Rev.* **2010**, *110*, 6891−6936.

(2) Smith, M. B.; Michl, J. Recent Advances in Singlet Fission. *Annu. Rev. Phys. Chem.* **2013**, *64*, 361−386.

(3) Miyata, K.; Conrad-Burton, F. S.; Geyer, F. L.; Zhu, X. Y. Triplet Pair States in Singlet Fission. *Chem. Rev.* **2019**, *119*, 4261−4292.

(4) Pensack, R. D.; Tilley, A. J.; Grieco, C.; Purdum, G. E.; Ostroumov, E. E.; Granger, D. B.; Oblinsky, D. G.; Dean, J. C.; Doucette, G. S.; Asbury, J. B.; Loo, Y.-L.; Seferos, D. S.; Anthony, J. E.; Scholes, G. D. Striking the right balance of intermolecular coupling for high-efficiency singlet fission. *Chem. Sci.* **2018**, *9*, 6240−6259.

(5) Pensack, R. D.; Ostroumov, E. E.; Tilley, A. J.; Mazza, S.; Grieco, C.; Thorley, K. J.; Asbury, J. B.; Seferos, D. S.; Anthony, J. E.; Scholes, G. D. Observation of Two Triplet-Pair Intermediates in Singlet Exciton Fission. *J. Phys. Chem. Lett.* **2016**, *7*, 2370−2375.

(6) Wilson, M. W.; Rao, A.; Clark, J.; Kumar, R. S.; Brida, D.; Cerullo, G.; Friend, R. H. Ultrafast dynamics of exciton fission in polycrystalline pentacene. *J. Am. Chem. Soc.* **2011**, *133*, 11830−11833.

(7) Lee, J.; Bruzek, M. J.; Thompson, N. J.; Sfeir, M. Y.; Anthony, J. E.; Baldo, M. A. Singlet exciton fission in a hexacene derivative. *Adv. Mater.* **2013**, *25*, 1445−1448.

(8) Trinh, M. T.; Pinkard, A.; Pun, A. B.; Sanders, S. N.; Kumarasamy, E.; Sfeir, M. Y.; Campos, L. M.; Roy, X.; Zhu, X. Y. Distinct properties of the triplet pair state from singlet fission. *Sci. Adv.* **2017**, *3*, e1700241.
(9) Breen, I.; Tempelaar, R.; Bizimana, L. A.; Kloss, B.; Reichman, D. R.; Turner, D. B. Triplet Separation Drives Singlet Fission after Femtosecond Correlated Triplet Pair Production in Rubrene. *J. Am. Chem. Soc.* **2017**, *139*, 11745−11751.
(10) Stern, H. L.; Cheminal, A.; Yost, S. R.; Broch, K.; Bayliss, S. L.; Chen, K.; Tabachnyk, M.; Thorley, K.; Greenham, N.; Hodgkiss, J. M.; Anthony, J.; Head-Gordon, M.; Musser, A. J.; Rao, A.; Friend, R. H. Vibronically coherent ultrafast triplet-pair formation and subsequent thermally activated dissociation control efficient endothermic singlet fission. *Nat. Chem.* **2017**, *9*, 1205.
(11) Stuart, A. N.; Tapping, P. C.; Schrefl, E.; Huang, D. M.; Kee, T. W. Controlling the Efficiency of Singlet Fission in TIPS-Pentacene/Polymer Composite Nanoparticles. *J. Phys. Chem. C* **2019**, *123*, 5813−5825.
(12) Folie, B. D.; Haber, J. B.; Refaely-Abramson, S.; Neaton, J. B.; Ginsberg, N. S. Long-Lived Correlated Triplet Pairs in a π-Stacked Crystalline Pentacene Derivative. *J. Am. Chem. Soc.* **2018**, *140*, 2326−2335.
(13) Herz, J.; Buckup, T.; Paulus, F.; Engelhart, J.; Bunz, U. H.; Motzkus, M. Acceleration of Singlet Fission in an Aza-Derivative of TIPS-Pentacene. *J. Phys. Chem. Lett.* **2014**, *5*, 2425−2430.
(14) Musser, A. J.; Liebel, M.; Schnedermann, C.; Wende, T.; Kehoe, T. B.; Rao, A.; Kukura, P. Evidence for conical intersection dynamics mediating ultrafast singlet exciton fission. *Nat. Phys.* **2015**, *11*, 352−357.
(15) Wong, C. Y.; Cotts, B. L.; Wu, H.; Ginsberg, N. S. Exciton dynamics reveal aggregates with intermolecular order at hidden interfaces in solution-cast organic semiconducting films. *Nat. Commun.* **2015**, *6*, 5946.
(16) Grieco, C.; Doucette, G. S.; Pensack, R. D.; Payne, M. M.; Rimshaw, A.; Scholes, G. D.; Anthony, J. E.; Asbury, J. B. Dynamic Exchange During Triplet Transport in Nanocrystalline TIPS-Pentacene Films. *J. Am. Chem. Soc.* **2016**, *138*, 16069−16080.
(17) Yost, S. R.; Lee, J.; Wilson, M. W. B.; Wu, T.; McMahon, D. P.; Parkhurst, R. R.; Thompson, N. J.; Congreve, D. N.; Rao, A.; Johnson, K.; Sfeir, M. Y.; Bawendi, M. G.; Swager, T. M.; Friend, R. H.; Baldo, M. A.; Van Voorhis, T. A transferable model for singlet-fission kinetics. *Nat. Chem.* **2014**, *6*, 492−497.
(18) Yong, C. K.; Musser, A. J.; Bayliss, S. L.; Lukman, S.; Tamura, H.; Bubnova, O.; Hallani, R. K.; Meneau, A.; Resel, R.; Maruyama, M.; Hotta, S.; Herz, L. M.; Beljonne, D.; Anthony, J. E.; Clark, J.; Sirringhaus, H. The entangled triplet pair state in acene and heteroacene materials. *Nat. Commun.* **2017**, *8*, 15953.
(19) Nie, Z.; Long, R.; Li, J.; Zheng, Y. Y.; Prezhdo, O. V.; Loh, Z.-H. Selective Excitation of Atomic-Scale Dynamics by Coherent Exciton Motion in the Non-Born−Oppenheimer Regime. *J. Phys. Chem. Lett.* **2013**, *4*, 4260−4266.
(20) Tayebjee, M. J. Y.; Schwarz, K. N.; MacQueen, R. W.; Dvořák, M.; Lam, A. W. C.; Ghiggino, K. P.; McCamey, D. R.; Schmidt, T. W.; Conibeer, G. J. Morphological Evolution and Singlet Fission in Aqueous Suspensions of TIPS-Pentacene Nanoparticles. *J. Phys. Chem. C* **2016**, *120*, 157−165.
(21) Pensack, R. D.; Grieco, C.; Purdum, G. E.; Mazza, S. M.; Tilley, A. J.; Ostroumov, E. E.; Seferos, D. S.; Loo, Y.-L.; Asbury, J. B.; Anthony, J. E.; Scholes, G. D. Solution-processable, crystalline material for quantitative singlet fission. *Mater. Horiz.* **2017**, *4*, 915−923.
(22) He, Z.; Xiao, K.; Durant, W.; Hensley, D. K.; Anthony, J. E.; Hong, K.; Kilbey, S. M., II; Chen, J.; Li, D. Enhanced Performance Consistency in Nanoparticle/TIPS Pentacene-Based Organic Thin Film Transistors. *Adv. Funct. Mater.* **2011**, *21*, 3617−3623.
(23) Herz, J.; Buckup, T.; Paulus, F.; Engelhart, J. U.; Bunz, U. H. F.; Motzkus, M. Unveiling Singlet Fission Mediating States in TIPS-pentacene and its Aza Derivatives. *J. Phys. Chem. A* **2015**, *119*, 6602−6610.
(24) Grieco, C.; Kennehan, E. R.; Kim, H.; Pensack, R. D.; Brigeman, A. N.; Rimshaw, A.; Payne, M. M.; Anthony, J. E.; Giebink, N. C.; Scholes, G. D.; Asbury, J. B. Direct Observation of Correlated Triplet Pair Dynamics during Singlet Fission Using Ultrafast Mid-IR Spectroscopy. *J. Phys. Chem. C* **2018**, *122*, 2012−2022.
(25) Pabst, M.; Köhn, A. Implementation of transition moments between excited states in the approximate coupled-cluster singles and doubles model. *J. Chem. Phys.* **2008**, *129*, 214101.
(26) Hellner, C.; Lindqvist, L.; Roberge, P. C. Absorption spectrum and decay kinetics of triplet pentacene in solution, studied by flash photolysis. *J. Chem. Soc., Faraday Trans. 2* **1972**, *68*, 1928−1937.
(27) Khan, S.; Mazumdar, S. Theory of Transient Excited State Absorptions in Pentacene and Derivatives: Triplet−Triplet Biexciton versus Free Triplets. *J. Phys. Chem. Lett.* **2017**, *8*, 5943−5948.
(28) Guo, D.; Ma, L.; Zhou, Z.; Lin, D.; Wang, C.; Zhao, X.; Zhang, F.; Zhang, J.; Nie, Z. Charge transfer dynamics in a singlet fission organic molecule and organometal perovskite bilayer structure. *J. Mater. Chem. A* **2020**, *8*, 5572−5579.
(29) Suna, A. Kinematics of Exciton-Exciton Annihilation in Molecular Crystals. *Phys. Rev. B* **1970**, *1*, 1716−1739.
(30) Kopelman, R. Fractal Reaction Kinetics. *Science* **1988**, *241*, 1620.
(31) Kim, H.; Keller, B.; Ho-Wu, R.; Abeyasinghe, N.; Vázquez, R. J.; Goodson, T.; Zimmerman, P. M. Enacting Two-Electron Transfer from a Double-Triplet State of Intramolecular Singlet Fission. *J. Am. Chem. Soc.* **2018**, *140*, 7760−7763.
(32) Chan, W. L.; Ligges, M.; Jailaubekov, A.; Kaake, L.; Miaja-Avila, L.; Zhu, X. Y. Observing the multiexciton state in singlet fission and ensuing ultrafast multielectron transfer. *Science* **2011**, *334*, 1541−1545.
(33) Bardeen, C. J. Time dependent correlations of entangled states with nondegenerate branches and possible experimental realization using singlet fission. *J. Chem. Phys.* **2019**, *151*, 124503.

https://dx.doi.org/10.1021/acs.jpcc.0c03566
J. Phys. Chem. C 2020, 124, 14503−14509